Bioorganic & Medicinal Chemistry 19 (2011) 798–806

Contents lists available at ScienceDirect

Bioorganic & Medicinal Chemistry

journal homepage: www.elsevier.com/locate/bmc

Intramolecular azo-bridge as a cystine disulfide bond surrogate: Somatostatin-14 and brain natriuretic peptide (BNP) analogs

Gil Fridkin [a,*], Theodosia Maina [b], Berthold A. Nock [b], Dan Blat [c], Vered Lev-Goldman [c], Yosef Scolnik [c], Aviva Kapitkovski [c], Yelena Vachutinsky [a], Yoram Shechter [a], Yaakov Levy [d]

[a] Department of Chemical Biology, The Weizmann Institute of Science, Rehovot 76100, Israel
[b] Molecular Radiopharmacy, I/R-RP, NCSR 'Demokritos' 15310 Ag, Paraskevi Attikis, Athens, Greece
[c] Department of Organic Chemistry, The Weizmann Institute of Science, Rehovot 76100, Israel
[d] Department of Structural Biology, The Weizmann Institute of Science, Rehovot 76100, Israel

ARTICLE INFO

Article history:
Received 16 September 2010
Revised 26 November 2010
Accepted 4 December 2010
Available online 13 December 2010

Keywords:
Azo-cyclization
Cyclic-azo peptides
Somatostatin
BNP

ABSTRACT

Cystine disulfide bond is a common feature in numerous biologically active peptides and proteins and accordingly its replacement by various surrogates presents a potential route to obtain analogs with improved pharmacokinetic characteristics. The purpose of the present study was to assess whether an azo-bridge can serve as such a surrogate. In view of the marked clinical significance of somatostatin and the brain natriuretic peptide (BNP) we choose these peptides as a model. Three cyclic-azo somatostatin analogs and three cyclic-azo BNP analogs were effectively prepared in solution through azo bond formation between *p*-amino phenylalanine and His or Tyr residues that were positioned in the peptide sequences in place of the native Cys residues. The peptides binding affinities to the sst_2 and ANP-receptor (NPR-A) expressed on rat acinar pancreating carcinoma AR4-2J cell membranes and HeLa cells, respectively, were examined. The somatostatin analogs displayed good to moderate affinities to the rat sst_2 in the nM range with best results obtained with peptide 2, that is, IC_{50} = 8.1 nM. Molecular dynamics simulations on these peptides suggests on a correlation between the observed binding potencies and the degree of conformational space overlapping with that of somatostatin. The BNP analogs exhibited binding affinities to the NPR-A in the nM range with best results obtained with BNP-1, that is, IC_{50} = 60 nM.

1. Introduction

Somatostatin (SST), also known as somatotropin release-inhibiting factor (SRIF) is a natural cyclic tetradecapeptide hormone originally discovered in and isolated from bovine hypothalamus.[1] SST was found to be expressed in brain and in most peripheral organs and tissues, including the gut, kidneys, submandibular glands, prostate and placenta. SST exhibits a wide range of diverse physiological activities, such as inhibition of growth hormone, glucagon and insulin secretion.[2] These effects are elicited after its binding to a family of G-protein coupled receptors (GPCR) of which at least five subtypes (sst_{1-5}) have been cloned.[3] SST receptors (sst_{1-5}) are over-expressed in various pathologies, most importantly, in cancers, for example, neuroendocrine tumors, breast carcinoma, neuroblastoma, pituitary adenoma, kidney, ovarian and thyroid cancer.[4,5] In view of the above SST holds significant potential for clinical applications and consequently, numerous peptide,[6,7] and non-peptide,[8] SST analogs, were synthesized and evaluated for their therapeutic use. With regard to peptides, in addition to 'traditional' structure-function studies involving sequence shortening, amino acids substitution and incorporation of D-amino acids,[6] emphasis was also directed to the replacement of the intramolecular cystine S–S bridge by other cyclization means. Cyclization was thus induced for example, by amide bond formation,[9,10] by disulfide formation using penicillamine,[11] or β-mercapto-β,β-pentamethylene propionic acid,[12] through lanthionine-related mean,[13] by RCM,[14] via backbone cyclization[15] and by backbone-metal-cyclization (BMC).[16]

The brain natriuretic peptide (BNP) is a natural occurring disulfide cyclic peptide hormone, which was originally isolated from the brain.[17] However, this 32-amino acid peptide, which belongs to the natriuretic peptides (NP) family, is considered a circulating hormone and is produced mainly in the cardiac ventricles.[17] The NP have a key role in the regulation of sodium and water balance and accordingly show cardiovascular, renal, hemodynamic, endocrine and mitogenic effects.[18] These diverse NP actions are mediated through interactions with their receptors, which are located on numerous tissues such as vasculature, renal artery and the central nervous system. At least 3 different subtypes of NP receptors (NPR) have been identified: ANP-receptor (NPR-A), BNP receptor

* Corresponding author at present address: Department of Organic Chemistry, The Israel Institute for Biological Research, Ness-Ziona, PO Box 19, 74100, Israel. Tel.: +972 8 9381741; fax: +972 8 9381548.
E-mail addresses: gilf@iibr.gov.il, GilFridkin@hotmail.com (G. Fridkin).

0968-0896/$ - see front matter © 2010 Elsevier Ltd. All rights reserved.
doi:10.1016/j.bmc.2010.12.014

(NPR-B) and CNP receptor (NPR-C). However, most of the NP biological effects are mediated through interactions with the NPR-A and NPR-B. BNP, specifically, acts via the NPR-A and NPR-C, similarly to ANP.[16]

Recently we have introduced a novel approach for the synthesis of cyclic peptides which is based on the formation of an intramolecular azo bond between diazotized *p*-amino phenylalanine and tyrosine or histidine residues located on the peptide backbone.[19] Linear peptide sequences were used to develop this concept.[19,20] Azo-cyclization, was however, never evaluated as an alternative mode of ring formation in mimics of naturally-occurring cyclic peptides. The azo bridge holds several interesting characteristics, such as hydrophobicity, rigidity and pH and light sensitivity, which may have marked effect on cyclic peptides activity, selectivity and metabolic stability. The light sensitivity feature was specifically utilized for the photomodulation of peptide conformations. For example, an azobenzene moiety that was introduced into a cyclic peptide derived from the somatostatin active core provided the ability to modulate between peptide conformations upon applying UV irradiation/heat.[21] Nevertheless, in these short peptide mimics which present only part of the native somatostatin sequence, the azo bond did not directly replace the cystine disulfide bond.

The purpose of the present study was to assess whether the azo bond can directly and effectively replace the abundant and important cystine disulfide bond in naturally-occurring cyclic peptide sequences. In view of the marked clinical significance of SST and BNP, and thus the need to diversify and enlarge the existing SST and BNP-peptide arsenal, we choose these peptides as a model.

2. Results and discussion

2.1. Synthesis of somatostatin analogs

To directly evaluate the above question we have incorporated our cyclization 'tools' namely, *p*-amino phenylalanine (Pap) and His/Tyr residues in place of the original cysteines at positions 3 and 14, respectively, and maintained the rest of the peptide sequences identical to native SST-14 (Table 1). Linear peptides were assembled on solid-support using a peptide synthesizer, while azo-cyclization was performed in solution (Scheme 1). Successful azo-cyclization, with no apparent formation of dimers or oligomers, was confirmed by means of HPLC (Fig. 1), mass spectrometry, amino acid analyses (Table 2), and by UV–vis absorption studies of the azo chromophor (Fig. 2). These studies suggested that the peptides were obtained as a mixture of cis/trans isomers.[22] Interestingly, the synthesis of the His-derived azo-bridged SST analog resulted in the generation of two isomers termed peptides 2 and 3 (7/3 ratio, respectively) which could be purified by HPLC. The possibility that peptides 2 and 3 (Scheme 1 and Fig. 3A), which showed identical mass, represent cis and trans isomers was explored by attempting to isomerise them using heat,[23] or irradiation.[24] As no shift was observed in the UV–vis absorption spectra of these peptides after these procedures, we concluded that the peptides are not cis/trans isomers but rather regioisomers presumably obtained through imidazole modification at both positions 2 and 5. Since peptide 2 was obtained in excess we assume it corresponds to formation of the azo-bridge via position 2 of the imidazole, which seems more approachable than position 5, which is relatively sterically hindered by the adjacent β-methylene group. The fact that the azo-His somatostatin did not exhibit spectral changes following irradiation may be due to internal hydrogen bonding involving the imidazolic proton and the vicinal nitrogen of the azo bond. Such association may contribute to the stability of a preferred conformer.[25] In the case of a phenyl-azo-phenyl structure this possibility does not exist.

Table 1
Cyclic-azo somatostatin peptides and their binding affinity to sst_2

Peptide	Sequence[a]	IC_{50}[b] (nM)
SST-14	A^1-G^2-Cys^3-K^4-N^{5}-F^6-F^7-W^8-K^9-T^{10}-F^{11}-T^{12}-S^{13}-Cys^{14} (S—S)	0.4 ± 0.1
1	A-G-Pap-K-N-F-F-W-K-T-F-T-S-His	ND
2	A-G-Pap-K-N-F-F-W-K-T-F-T-S-His	8.1 ± 1.7
3	A-G-Pap-K-N-F-F-W-K-T-F-T-S-His	44.0 ± 6.9
4	A-G-Pap-K-N-F-F-W-K-T-F-T-S-Tyr	ND
5	A-G-Pap-K-N-F-F-W-K-T-F-T-S-Tyr	>600

ND—not determined.
[a] Pap—*p*-amino phenylalanine; the connected line between Pap and His/Tyr represents the azo bridge.
[b] Peptide concentrations producing 50% inhibition of [^{125}I-Tyr^3]octreotide binding.

2.2. Binding affnity of the somatostatin analogs

The binding affinity of the three cyclic-azo peptides to the sst_2 expressed on rat acinar pancreating carcinoma AR4-2J cell membranes was next determined.[26] As shown in the comparative displacement curves (Fig. 4), the peptides displayed good to moderate affinities for the rat sst_2 (Table 1). Peptide 2 (IC_{50} = 8.1 nM) and 3 (IC_{50} = 44.0 nM), that is, the two azo-His isomers, inhibited the binding of [^{125}I-Tyr^3]octreotide in a monophasic and dose-dependent manner, while peptide 5 (IC_{50} >600 nM), that is, azo-Tyr, marginally interacted with the receptor.

2.3. Molecular dynamics of the somatostatin analogs

In an attempt to understand this difference in binding affinities we have performed molecular dynamics simulations on these peptides aiming at capturing their available conformational space. Accordingly, SST-14 and its five synthesized variants (Table 1) were simulated at high temperatures; for each peptide five hundred conformations were sampled, and were gradually cooled down to represent conformations at very low temperatures. These conformations, which may represent the most accessible basins of the potential energy landscape, were then mapped using the Principal Component Analysis (PCA) method[27] to allow the projection of the multidimensional conformational space of the peptides on the same collective coordinate. The projected conformational spaces show that the cyclization of SST significantly shrinks the available conformational space of the peptide (Fig. 5). Peptides 2 and 3, which have the same sequence but differ only in the atoms of His14 through which the azo-bridge is formed, have similar conformational spaces as the overlap between their projected conformational spaces is about 90%. In addition, it was found that cyclic peptides 2 and 3 hold a smaller conformational space than peptide 5 and present better overlapping, that is, of 73% and 66%, respectively, with the conformational space sampled by SST-14 as compared to peptide 5, which showed 48% overlap (Fig. 5). Peptides 2 and 3 differ from peptide 5 only in the identity of the residue at position 14, yet show marked difference in binding activity. The overlap between the conformational space of peptides 3 and 5 is of 72% (Fig. 5C and D). The relative bioactivity[27a] (calculated by $[-\log(IC_{50})]^{peptide}/[-\log(IC_{50})]^{SST\text{-}14}$) of peptides 2, 3, and 5 is 86%, 79%, and 66%, respectively. Namely, the relative bioactivity correlates well with the degree of overlap between the conformational space sampled by these peptides and by SST-14. Accordingly, we propose that the identity of the residues can affect the flexibility of the peptide, the allowed conformational space and thus the ability to obtain the bioactive conformation.

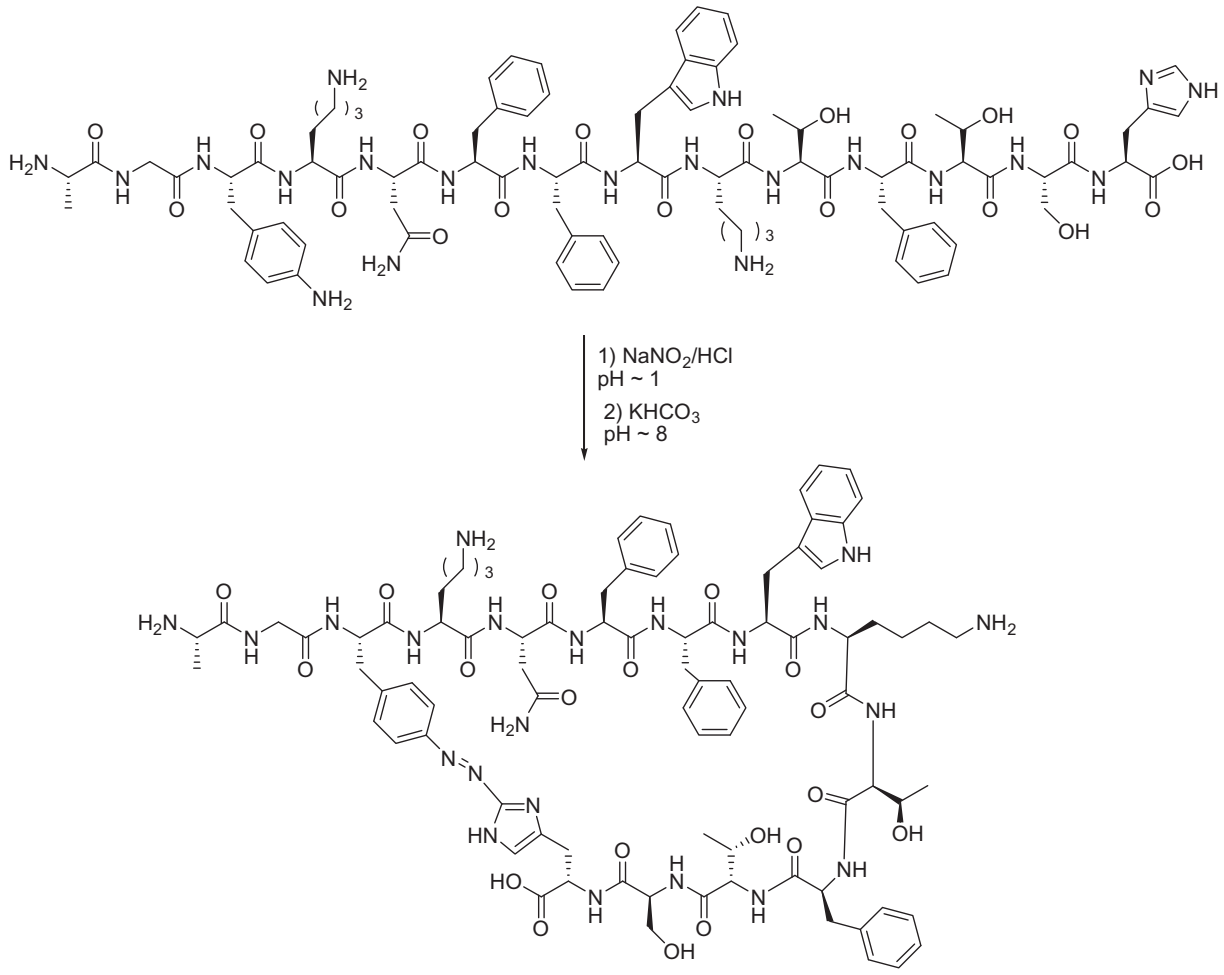

Scheme 1. Synthesis of peptide 2, a SST-14 mimic, by azo cyclization through *p*-amino phenylalanine and an histidine residue; diazotation at C-2 of the imidazole.

2.4. Synthesis of BNP analogs

Following the same rational applied in the somatostatin mimics design, in the case of BNP the Tyr and Pap residues were incorporated in place of the native Cys residues at positions 10 and 26, respectively, while the rest of the peptide sequence was left unchanged (Table 3). In this manner the effect of azo-cyclization could be evaluated directly. The 32-amino acid long linear peptide was assembled, as before, on solid-support using a peptide synthesizer, while azo-cyclization was performed in solution following similar experimental protocols as mentioned above (Scheme 2). The crude peptide was then purified by HPLC to furnish three different fractions that hold the desired molecular weight (Table 3). Subjecting these samples to amino acid analyses revealed that the main fraction (>80%) termed BNP-1 is the desired cyclic peptide, which is obtained through azo bond formation between the Tyr^{10} and Pap^{26} residues (Scheme 2). The second fraction however, obtained in ~15% termed BNP-2 is derived from azo-cyclization between the Pap^{26} residue and the native His^{32} residue located at the peptide C-terminus (Fig. 6). The feasibility of azo-cyclization between these rather close residues, which is evident by the absence of an His and the presence of a Tyr residue in the amino acid analysis, was further supported by the amino acid analysis of the third fraction (BNP-3, <5%) which gave the same results. The formation of two cyclic azo peptides from one linear sequence holding both Tyr and His residues was observed by us previously in the synthesis of azo cyclic GnRH analogs.[20] It appears that similar to the case of GnRH, in the case of BNP the distance between the Tyr/His and Pap residues was the major parameter affecting the propensity of the peptide to close by either residue. Evidently, in the synthesis of both GnRH and BNP the products with the larger rings were obtained in significant higher yields. In addition, it appears that like in the case of somatostatin, once a His residue is present azo-cyclization can occur by either the imidazole 2 (BNP-2) or 5 position (BNP-3).

2.5. Binding affinity of the BNP analogs

The binding affinity of the two major cyclic-azo BNP peptides (BNP 1,2) as well as native BNP to the NPR-A expressed on HeLa cell membranes was next examined using a compettion binding assay with [^{125}I]ANP as the radioligand. As can be seen in Table 3 BNP-1 was found to be the most active binder with an IC_{50} value of 60 nM, which is only 10 times less active than native BNP (6 nM). BNP-2 was however, a four times less active binder than BNP-1 exhibiting an IC_{50} value of 240 nM. As mentioned before, BNP-1 and 2 differ in the location of the azo bridge. While in BNP-1 it is located between Tyr^{10} and Pap^{26} which is the exact position of the native disulfide bond in BNP, in BNP-2 the bridge is placed between the Pap and His residues located in positions 26 and 32, respectively. It is reasonable to hypothesize that due to BNP-1 similarity to BNP it may obtain conformations that closely resemble the bioactive conformation exhibited by the latter while for BNP-2 this process is less favoured.

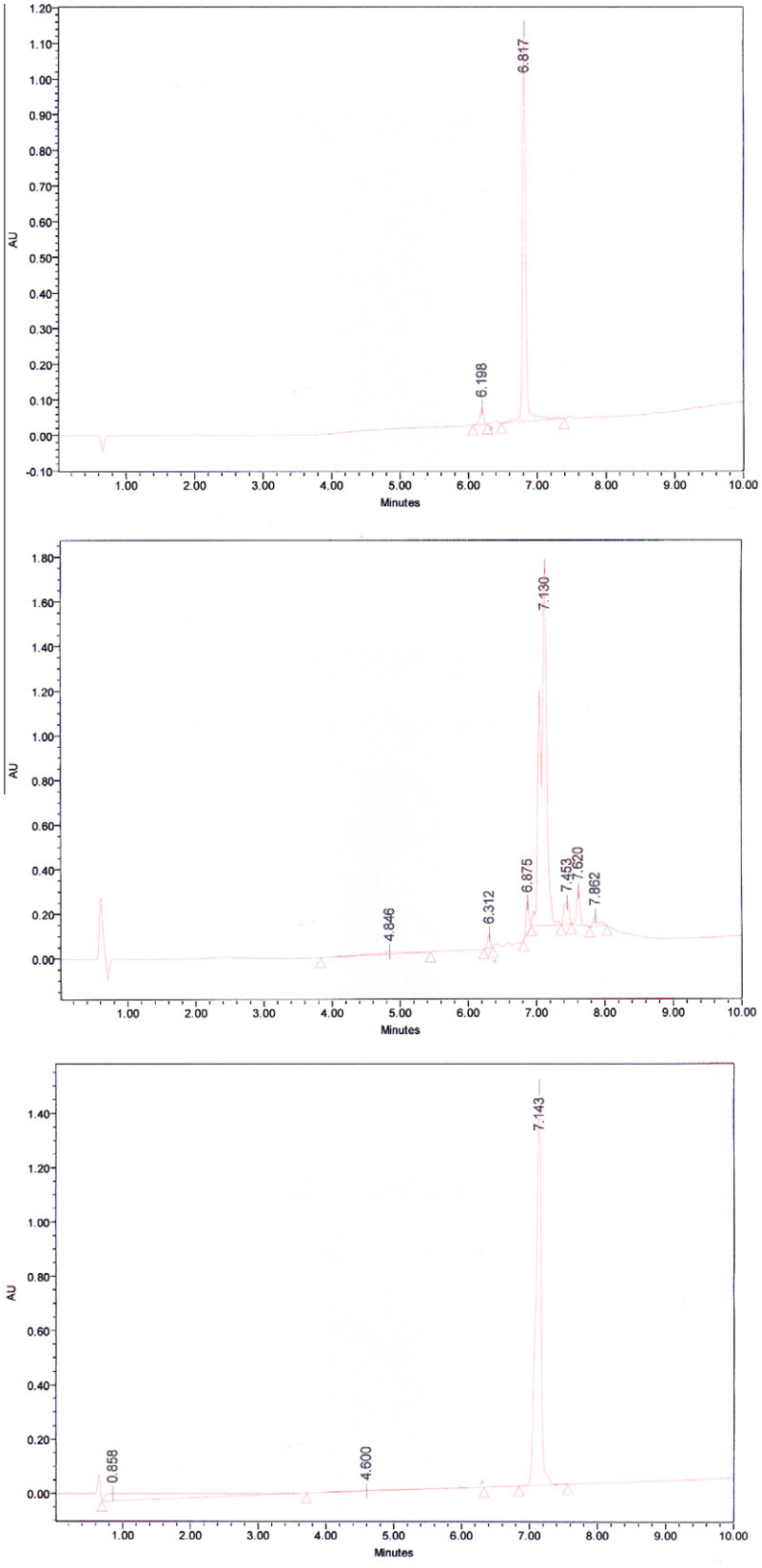

Figure 1. HPLC spectra of somatostatin peptides. (A) crude peptide 1, the linear precursor of cyclic peptides 2 and 3. (B) Crude cyclic peptides 2 and 3. (C) Purified peptide 3.

Table 2
Amino acid composition of synthesized somatostatin peptides[a]

Peptide No.	Ala	Gly	Lys	Asp	Phe	Thr	Ser	Tyr	His
1	(1) 0.99	(1) 1.00	(2) 2.04	(1) 1.04	(3) 3.14	(2) 1.99	(1) 0.93	–	(1) 1.04
2	(1) 0.95	(1) 1.00	(2) 1.94	(1) 0.90	(3) 2.93	(2) 1.91	(1) 0.83	–	(1) 0.07
3	(1) 0.97	(1) 1.00	(2) 1.85	(1) 0.90	(3) 2.96	(2) 1.90	(1) 0.87	–	(1) 0.06
4	(1) 0.99	(1) 1.00	(2) 2.00	(1) 1.06	(3) 3.14	(2) 1.99	(1) 0.90	(1) 0.99	–
5	(1) 1.00	(1) 1.00	(2) 1.88	(1) 1.02	(3) 3.08	(2) 1.95	(1) 0.88	(1) 0.07	–

[a] *p*-Aminophenylalanine and tryptophan were not determined.

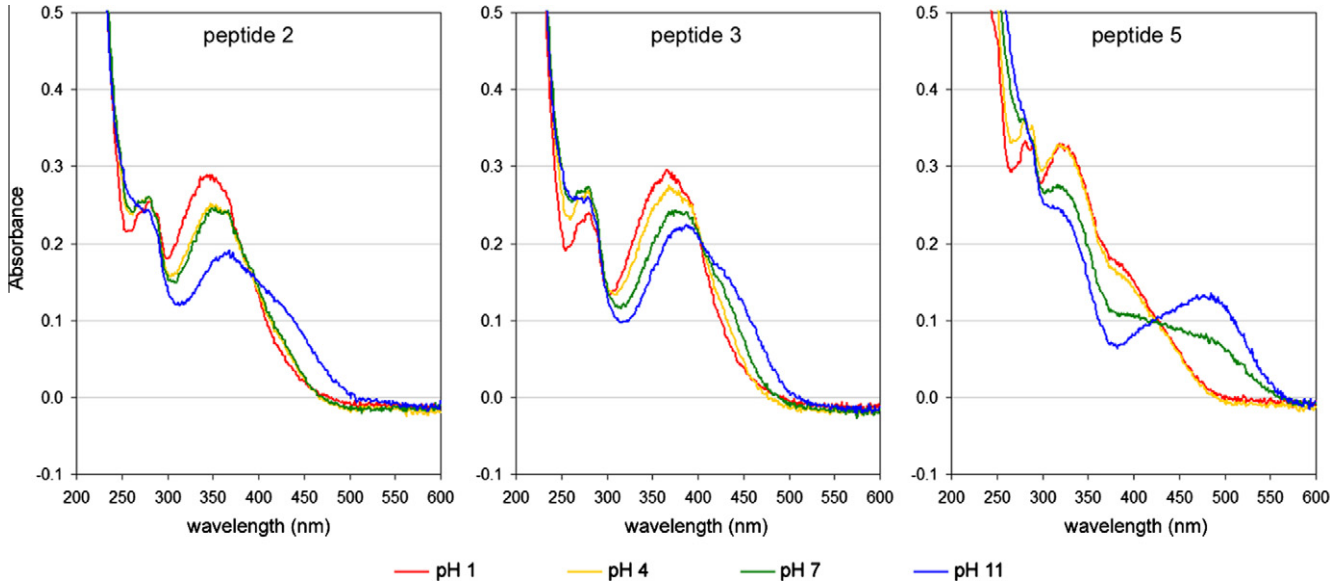

Figure 2. UV absorption spectra of the cyclic azo-bridged somatostatin analogs in different pH conditions.

3. Conclusion

The feasibility of utilizing azo-bridge as a cystine disulfide bond surrogate was shown through the synthesis and binding studies of SST-14 and BNP mimetics. As the purpose of the present study was to conceptually evaluate if these peptides preserve substantial biological potency, no attempts were made to optimize the formation of a specific conformer. Thus the affect of parameters like concentration, pH and reaction temperature were not investigated. It is reasonable to assume that the nature of the azo bond as well as its location on the imidazole ring may vary from peptide to peptide depending, for example, on intramolecular/intermolecular interactions such as charge-charge, hydrophobic and hydrogen bonding. Numerous biologically active peptides of high therapeutic-diagnostic potential possess cystine disulfide bonds, accordingly, we believe that the present findings with somatostatin and BNP have diverse and wide implications beyond these model peptides.

4. Experimental

4.1. Materials and methods

All chemicals and reagents were of analytical grade. Resins, Fmoc-protected amino acid derivatives and all reagents for solid-phase synthesis were obtained from Novabiochem (Laufelingen, Switzerland). Side-chain protecting groups employed were as follows: Arg, 2,2,4,6,7-pentamethyl-dihydrobenzofuran-5-sulfonyl (Pbf); His, Trt; Trp and *p*-amino phenylalanine, BOC; Ser and Tyr; *tert*-butyl (*t*-Bu). Reverse-phase HPLC was performed on a Spectra-Physics SP-8800 liquid chromatography system equipped with an Applied Biosystems 757 variable wavelength absorbance detector. HPLC pre-packed columns used were: Lichrocart, containing Lichrospher RP-18 (250 × 10 mm; 7 μm) for semi-preparative purification and Lichrospher 100 RP-18 (250 × 4 mm; 5 μm) for analytical purposes (Merck, Darmstadt, Germany). HPLC purification and analyses were achieved by using gradients formed from 0.1% TFA in water as solvent A and 0.1% TFA in 75% aqueous MeCN as solvent B. Eluent composition was 10% B in A for the first 10 min and increased linearly to 100% B, 50 min after injection time. Flow rates were 1 ml/min and 10 ml/min for analytical and preparative purposes, respectively. The column effluents were monitored by UV absorbance at 214 nm. Mass analyses were performed using MALDI-TOF and ESI-MS techniques (Bruker-Reflex-Reflection model, Germany, and VG-platform-II electrospray single quadruple mass spectrometer, Micro Mass, UK, respectively). For amino acid composition evaluations peptides were hydrolyzed in 6 N HCl at 100 °C for 24 h under vacuum, and the hydrolyzates were analyzed with a Dionex Automatic Amino Acid Analyzer. The rat pancreatic tumor cell line AR4-2J was kindly provided by Dr. R. Kleene (Philipps University, Marburg, Germany). All culture media were supplied by Gibco BRL, Life Technologies (Grand Island, NY) and all supplements by Biochrom KG Seromed® (Berlin, Germany). For protein measurements the protein microdetermination kit (Procedure No. P 5656) by SIGMA Diagnostics (St. Louis, USA) was utilized. Iodine-125 was purchased from MDS Nordion, SA (Fleurus, Belgium). [Tyr^3]octreotide was a kind gift from the IAEA whereas SST-14 was purchased from Sigma–Aldrich (Athens, Greece). Radioiodination of [Tyr^3]octreotide was performed following a modification of a published protocol.[26,28] For radioactivity measurements an automatic

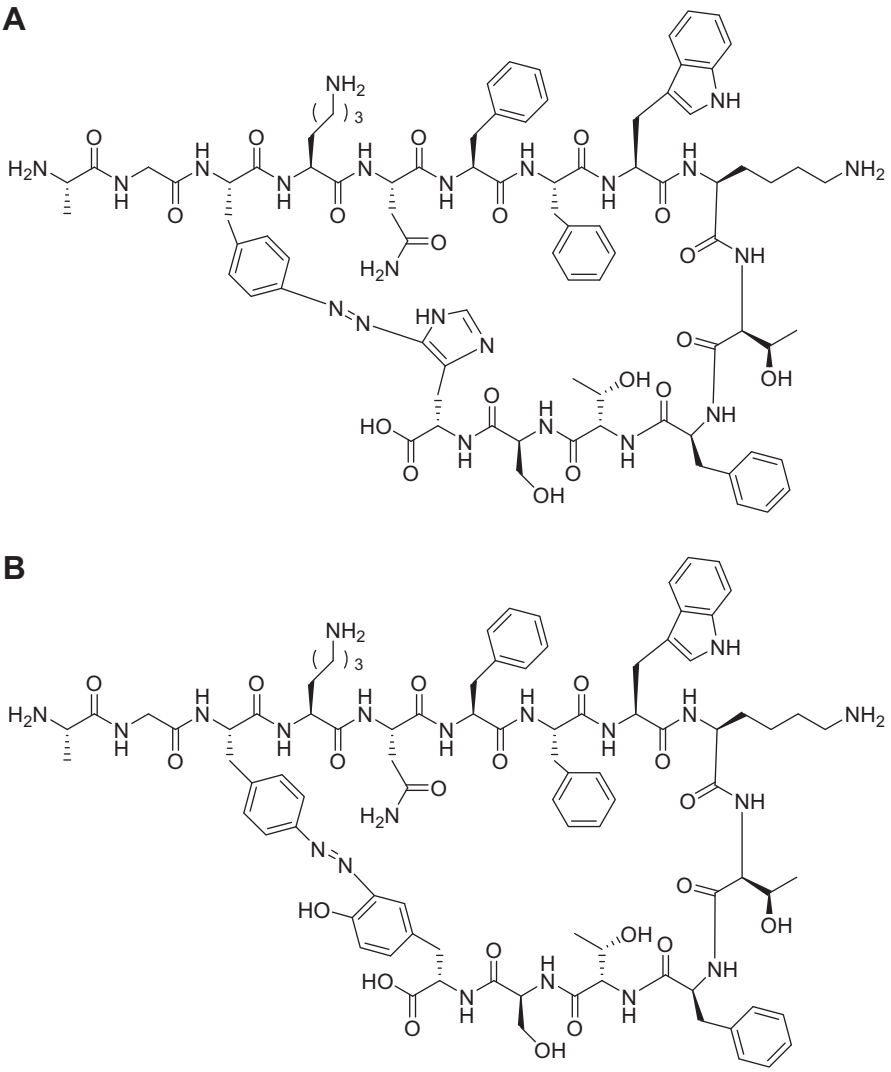

Figure 3. Schematic representation of somatostatin cyclic azo mimics. (A) Peptide 3. (B) Peptide 5.

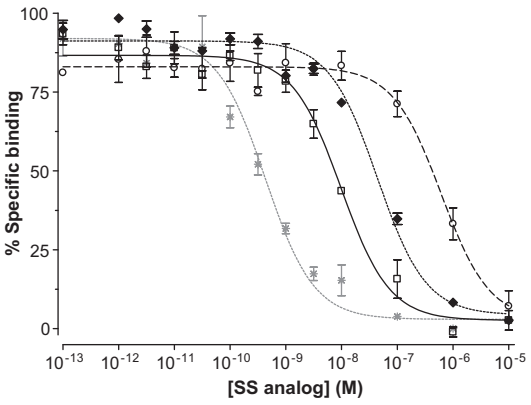

Figure 4. Competitive inhibition of [^{125}I-Tyr^3]octreotide binding to sst_2 expressed on AR4-2J cell membranes by increasing concentrations of SST-14 (∗), peptide 2 (□), peptide 3 (♦), and peptide 5 (o).

well-type gamma counter was used [NaI(Tl) crystal, Canberra Packard Auto-Gamma 5000 series instrument]. A Brandel M-48 Cell Harvester (Adi Hassel Ingenieur Büro, Munich, Germany) was employed in the binding experiments.

4.2. Somatostatin peptide synthesis

The pre-cyclic linear peptides were prepared on solid-support (Wang resin, Novabiochem, Laufelingen, Switzerland) with an APEX 396 synthesizer (Advanced ChemTech, Louisville, KY, USA) using Fmoc chemistry, following the company's protocols. All synthesized peptides were simultaneously deprotected/cleaved from the resin using a solution of TFA/triethylsilane/water (17:1:1). After 2 h at room temperature, the cleaved mixtures were filtered and the peptides were precipitated from the solutions with peroxide-free dry methyl *t*-butyl ether at 0 °C. Precipitated peptides were washed with cold ether, dissolved in water and lyophilized. The crude peptides (>85% pure) were directly used, without further purification for azo-cyclization as described before.[19,20] Briefly, the corresponding lyophilized peptide powders (5–50 mg) were dissolved in 0.1 M HCl (50 μL per mg peptide) and the solutions were cooled to 0 °C. A cooled aqueous sodium nitrite solution (0.1 M) was then added portion-wise to achieve a 1:1 peptide/nitrite molar ratio and the reaction mixtures were allowed to stand with occasional mixing for 10 min at 0 °C. They were then added, portion-wise, to an ice-cold 0.1 M $KHCO_3$ solution (2 ml per 1 mg peptide), and the reaction mixtures, following adjustment of their pH to 8.0 by addition of 1 M K_2CO_3, were kept for 3–4 h in the cold, followed by overnight incubation at room temperature. The homogenous

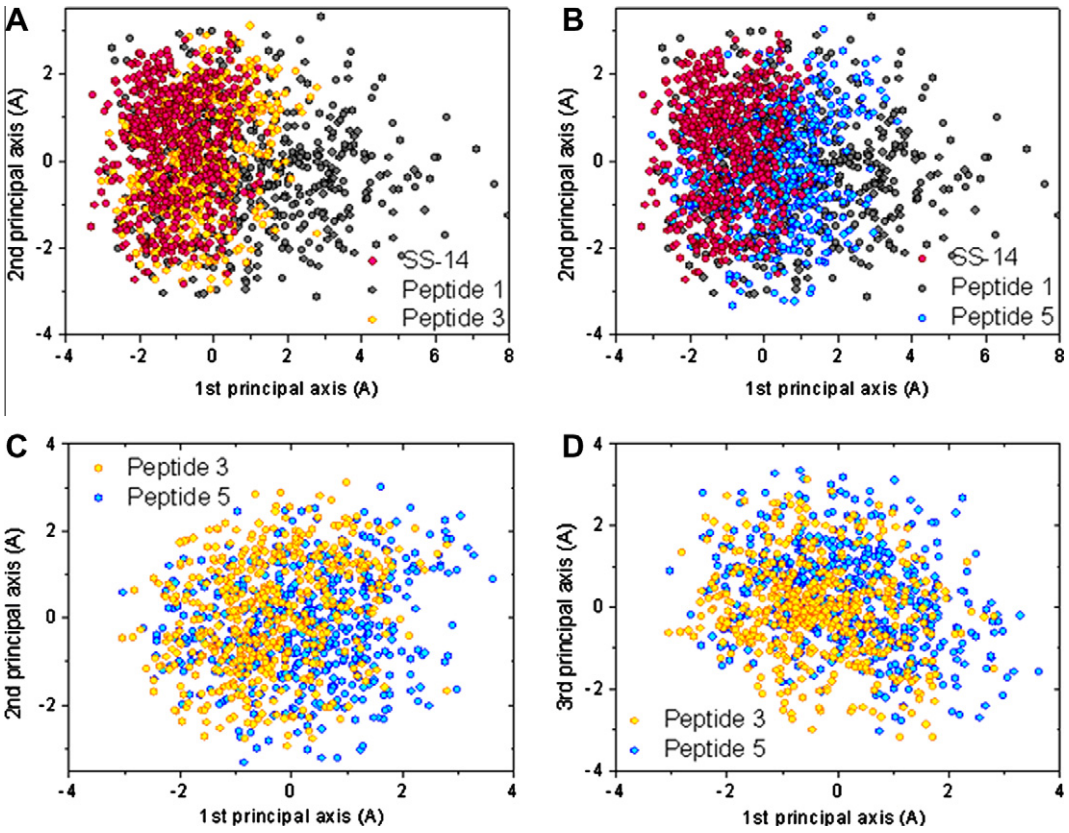

Figure 5. A joint projection of the conformational space of SST-14 and some of its variants on two principal axes. Each point represents a single conformation among the 500 conformations that represent the conformational space of each peptide. (A) Comparison between the conformational space of peptides 1, 3, and SST-14. (B) Comparison between the conformational space of peptides 1, 5, and SST-14. (C) Comparison of the conformational space of peptides 3 and 5 using the first two principal axes. (D) Comparison of the conformational space of peptides 3 and 5 using the first and third principal axes.

Table 3
Cyclic-azo BNP peptides and their binding affinity to NPR-A

Peptide	Sequence[a]	IC_{50}[b] (nM)
BNP	S^1-P^2-K^3-M^4-V^5-Q^6-G^7-S^8-G^9-**C^{10}**-F^{11}-G^{12}-R^{13}-K^{14}-M^{15}-D^{16}-R^{17}-I^{18}-S^{19}-S^{20}-S^{21}-S^{22}-G^{23}-L^{24}-G^{25}-**C^{26}**-K^{27}-V^{28}-L^{29}-R^{30}-R^{31}-H^{32}	6
BNP-1	S^1-P^2-K^3-M^4-V^5-Q^6-G^7-S^8-G^9-**Y^{10}**-F^{11}-G^{12}-R^{13}-K^{14}-M^{15}-D^{16}-R^{17}-I^{18}-S^{19}-S^{20}-S^{21}-S^{22}-G^{23}-L^{24}-G^{25}-**Pap^{26}**-K^{27}-V^{28}-L^{29}-R^{30}-R^{31}-H^{32}	60
BNP-2	S^1-P^2-K^3-M^4-V^5-Q^6-G^7-S^8-G^9-T^{10}-F^{11}-G^{12}-R^{13}-K^{14}-M^{15}-D^{16}-R^{17}-I^{18}-S^{19}-S^{20}-S^{21}-S^{22}-G^{23}-L^{24}-G^{25}-**Pap^{26}**-K^{27}-V^{28}-L^{29}-R^{30}-R^{31}-**H^{32}**	240
BNP-3	S^1-P^2-K^3-M^4-V^5-Q^6-G^7-S^8-G^9-T^{10}-F^{11}-G^{12}-R^{13}-K^{14}-M^{15}-D^{16}-R^{17}-I^{18}-S^{19}-S^{20}-S^{21}-S^{22}-G^{23}-L^{24}-G^{25}-**Pap^{26}**-K^{27}-V^{28}-L^{29}-R^{30}-R^{31}-**H^{32}**	ND

ND—not determined.
[a] Pap—*p*-amino phenylalanine; letters in bold represent points of cyclization; in the case of BNP, cyclization is via a disulfide bond while in the case of BNP-1-3 cyclization is through an azo bridge.
[b] Peptide concentrations producing 50% inhibition of [^{125}I]ANP binding.

solutions gradually turned brownish-orange or yellowish upon standing. Lyophilization resulted in yellowish-brown powdered crude cyclic peptides, which were further purified by semi-preparative HPLC. Lyophilized, isolated peptides were evaluated by analytical HPLC, amino acid analysis and mass spectroscopy. Analyses revealed high purities (>97%) of the cyclic peptides and confirmed their identity, respectively. Mass spectrometry (m/z): Peptide 2; calcd. $[M+H]^+$ = 1744.96; found $[M+H]^+$ = 1745.03. Peptide 3; calcd $[M+H]^+$ = 1744.96; found $[M+H]^+$ = 1744.98. Peptide 5; calcd $[M+H]^+$ = 1770.99; found $[M+H]^+$ = 1771.42.

4.3. UV–vis absorption studies

Lyophilized pure peptides were dissolved in double-distilled water to obtain 50 mM solutions. Different pH values were obtained by titration with minute volumes of concentrated HCl or NaOH, until the target pH was observed. Each solution was then scanned for UV–vis absorption over the spectrum of 200–600 nm (Fig. 2) using a Varian Cary 50 UV–vis spectrophotometer (Palo Alto, CA, USA).

4.4. Attempted isomerization of the azo bond

The possibility that peptides 2 and 3 represent *cis* and *trans* isomers was explored by an attempt to isomerise them using heat (50 °C for 12 h). Following this treatment the UV–vis absorption spectra of these peptides were examined, however, no shift was observed. The two peptides (50 μM) were than dissolved in 100 mM phosphate buffer (pH 7.0) and irradiated for 3 h at 25 °C using an electronic projector lamp (KL1500, Scott, Germany) equipped with filters, having a band pass of 320–510 nm with a λ_{max} of 400 nm. Following that procedure the UV–vis absorption spectra of the peptides were examined, however, as before, no shift was observed.

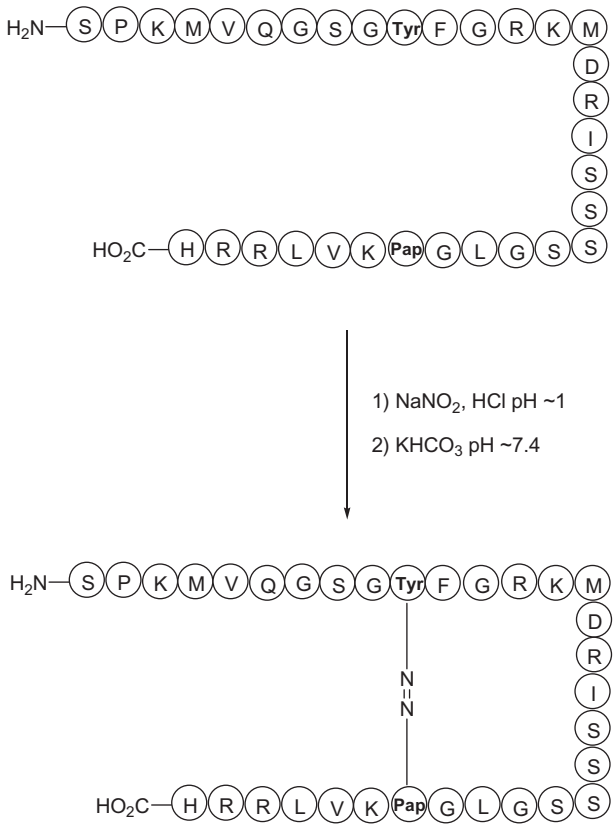

Scheme 2. Synthesis of BNP-1, a BNP mimic, by azo cyclization through *p*-amino phenylalanine and tyrosine residues (presented in bold).

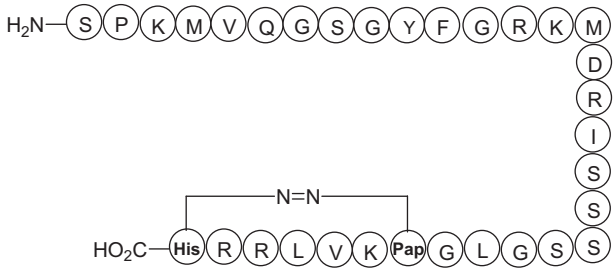

Figure 6. Schematic representation of BNP-2 and 3. BNP-2, diazotation at C-2 of the His imidazole; BNP-3, diazotation at C-5 of the His imidazole.

4.5. Receptor binding

4.5.1. Cell culture

Rat acinar pancreatic carcinoma AR4-2J cells predominantly expressing the sst_2[29] were maintained in Ham's F-12K nutrient mixture supplemented by 20% (v/v) fetal bovine serum, 2 mM glutamine, 100 U/mL penicillin and 100 μg/mL streptomycin, and grown to confluence in humidified air containing 5% CO_2 at 37 °C. Sub-culturing was performed once a week employing a trypsin/EDTA (0.05%/0.02% w/v) solution.

4.5.2. Preparation of AR4-2J cell membranes

AR4-2J cell membranes were collected according to a reported protocol.[30] In brief, AR4-2J cells were grown to confluence, mechanically disaggregated, washed twice with cold PBS buffer pH 7.0 and resuspended in homogenization buffer (1 mL/flask) containing 10 mM Tris pH 7.4 and 0.1 mM EDTA. Cells were homogenized using a Bioblock Scientific homogenizer (50 strokes/5 mL) and the homogenized suspension was centrifuged at 2600 rpm for 10 min at 4 °C in a J2-MC Beckman centrifuge. The supernatant was removed and recentrifuged at 26,000 rpm for 15 min at 4 °C in a CS120GX micro ultracentrifuge (Hitachi). The pellet was resuspended in homogenization buffer (100 μL/flask) and stored at −80 °C in aliquots of 100 μL. The protein concentration of the samples was determined according to the method of Lowry[31] using bovine serum albumin as the standard.

4.5.3. Binding assay

Competition binding experiments were performed according to a published protocol[26] using [^{125}I-Tyr^3]octreotide[28] (2200 Ci/mmol) as the radioligand and SST-14 as control peptide. Briefly, AR4-2J cell membrane homogenate, corresponding to 15 μg protein, was incubated with 30,000 cpm of radioligand in the presence of increasing concentrations of tested peptide in a total volume of 300 mL of HEPES buffer (50 mM HEPES pH 7.6, 0.3% BSA, 5 mM $MgCl_2$, 10 μM bacitracin) for 40 min at 37 °C. Analysis was performed by non-linear regression according to an one-site model employing the PRISM™ 2 program (GraphPad Software, San Diego, CA).

4.6. Molecular dynamics

To capture the conformational space of the peptides and the effects of the constraints on their flexibility, each system was simulated using molecular dynamics simulations at high temperatures (1000 K) for 5 ns. Along this high T trajectory, for each peptide 500 conformations were sampled and were gradually cooled down to represent conformations at very low temperatures. The high T trajectory allows crossing high barriers in the energy landscapes of the peptides. The 500 conformations may represent the most accessible basins of the potential energy landscape. Once 500 conformations were selected for each peptide, they were mapped using the Principal Component Analysis (PCA) method.[27]

4.7. BNP peptides synthesis

The linear peptide was assembled and cleaved from the resin as described above for the somatostatin analogs. For azo cyclization, the lyophilized peptide (3.6 mg, 1 μmol) was dissolved in 100 μL HCl (0.1 M) and the solution was cooled to 0 °C using an ice bath. A cooled aqueous sodium nitrite solution (10 μL, 0.1 M) was then added portion-wise to the peptide solution and the reaction mixture was vortexed, left in the cold for 5 min and then added, portion-wise, to an ice-cold $KHCO_3$ solution (30 ml, 0.03 M). The resulting reaction mixture, following adjustment of its pH to 7.4 by addition of 1 M K_2CO_3, was then kept for 1 h in the cold and 5 h at room temperature. Lyophilization of the solution resulted in yellowish powdered crude cyclic peptide, which was purified by semi-preparative HPLC (a gradient of 0–70% B over 50 min). Isolated peptides were evaluated by analytical HPLC, amino acid analysis and mass spectroscopy. Analyses revealed high purities (>97%) of the cyclic peptides and confirmed their identity, respectively.

4.8. Receptor binding

4.8.1. Cell culture

NPR-A expressing HeLa cells were grown at 35 °C in a 5% CO_2 humidified incubator in Dulbecco's modified Eagle's medium (DMEM) containing 10% fetal calf serum, penicillin and streptomycin (100 U/mL of each). The binding assay was performed on subconfluent cell monolayers in 24-well dishes at a density of 3×10^5 cells/well preincubated for 24 h.

4.8.2. Competition binding assay

HeLa cell monolayers were washed twice with PBS buffer (pH 7.4) containing 1% Bovine Serum Albumin and then incubated in the same buffer containing [^{125}I]ANP (100,000 cpm/well) and increasing concentrations (1–2000 ng/mL) of either native BNP or azo cyclic BNP derivatives for 2 h at 4 °C. Two wells did not contain BNP to allow the determination of total binding of [^{125}I]ANP alone. Non-specific binding was measured in the presence of an excess native BNP (20 μg/mL) The cells were then washed twice with ice-cold buffer, and solubilized with 0.2% w/v sodium dodecylsulphate (SDS). Following incubation (37 °C for 30 min), the solubilized cells were transferred to counting vials and counted for their radioactive content (γ-counter, Packard Cobra, GMI, USA). All experiments were performed in duplicates. Specific binding is defined as total radioactive content (in the absence of native BNP) minus that obtained at high (20 μg/mL) concentration of native BNP. Receptor binding capacity is determined by calculating the concentration of native BNP or its derivative that is required to displace 50% of specifically bound [^{125}I]ANP.

References and notes

1. Brazeau, P.; Vale, W.; Burgus, R.; Ling, N.; Butcher, M.; Rivier, J.; Guillemin, R. *Science* **1973**, *179*, 77–79.
2. Guillemin, R.; Gerich, J. E. *Ann. Rev. Med.* **1976**, *27*, 379.
3. Reisine, T.; Bell, G. I. *Endocr. Rev.* **1995**, *16*, 427–442.
4. Reubi, J. C. *Endocr. Rev.* **2003**, *24*, 389.
5. Froidevaux, S.; Eberle, A. N. *Biopolymers* **2002**, *66*, 161.
6. Grace, C. R. R.; Erchegyi, J.; Koerber, S. C.; Reubi, J. C.; Rivier, J.; Riek, R. *J. Med. Chem.* **2006**, *49*, 4487.
7. Janecka, A.; Zubrzyca, M.; Janecki, T. *J. Pept. Res.* **2001**, *58*, 91.
8. Rohrer, S. P. et al *Science* **1998**, *282*, 737.
9. Veber, D. F.; Holly, F. W.; Nutt, R. F.; Bergstrand, S. J.; Brady, S. F.; Hirschmann, R.; Glitzer, M. S.; Saperstein, R. *Nature* **1979**, *280*, 512.
10. Veber, D. F.; Freidinger, R. M.; Perlow, D. S.; Paleveda, W. J., Jr.; Holly, F. W.; Strachan, R. G.; Nutt, R. F.; Arison, B. H.; Homnick, W. C.; Randall, M. S.; Glitzer, M. S.; Saperstein, R.; Hirschmann, R. *Nature* **1981**, *292*, 55.
11. Pelton, J. T.; Gulya, K.; Hruby, V. J.; Duckles, S. P.; Yamamura, H. I. *Proc. Natl. Acad. Sci. U.S.A.* **1985**, *82*, 236.
12. Baranowska, B.; Radzikwska, M.; Wasilewska-Dziubinska, E.; Plonowski, A.; Roguski, K.; Legowska, A.; Przybylski, J. *Neuro. Endocrinol. Lett.* **1999**, *20*, 237.
13. Melacini, Q.; Zhu, G.; Osapay; Goodman, M. *J. Med. Chem.* **1997**, *40*, 2252.
14. D' Addona, D.; Carotenuto, A.; Novellino, E.; Piccand, V.; Reubi, J. C.; Di Cianni, A.; Gori, F.; Papini, A. M.; Ginaaeschi, M. *J. Med. Chem.* **2008**, *51*, 512.
15. Gilon, C.; Huenges, M.; Matha, B.; Gellerman, G.; Hornik, V.; Afargan, M.; Amitlay, O.; Ziv, O.; Feller, E.; Gamliel, A.; Shohat, D.; Wanger, M.; Arad, O.; Kessler, H. *J. Med. Chem.* **1998**, *41*, 919.
16. Fridkin, G.; Bonasera, T. A.; Litman, P.; Gilon, C. *Nucl. Med. Biol.* **2005**, *32*, 39.
17. Ogawa, Y.; Nakao, K.; Mukoyama, M.; Hosoda, K.; Shirakami, G.; Arai, H.; Saito, Y.; Suga, S.; Jougasaki, M.; Imura, H. *Circ. Res.* **1991**, *69*, 491–500.
18. Abassi, Z.; Karram, T.; Ellaham, S.; Winaver, J.; Hoffman, A. *Pharmacol. Ther.* **2004**, *102*, 223–241.
19. Fridkin, G.; Gilon, C. *J. Pept. Res.* **2002**, *60*, 104.
20. Fridkin, G.; Rahimipour, S.; Ben-Aroya, N.; Kapitkovsky, A.; Di-Segni, S.; Rosenberg, M.; Kustanovich, I.; Koch, Y.; Gilon, C.; Fridkin, M. *J. Pept. Sci.* **2006**, *12*, 106.
21. Ulysse, L. G., Jr.; Chmielewski, J. *Chem. Biol. Drug Des.* **2006**, *67*, 127.
22. Behrendt, R.; Renner, C.; Schenk, M.; Wang, F.; Wachtveitl, J.; Oesterhelt, D.; Moroder, L. *Angew. Chem., Int. Ed.* **1999**, *38*, 2771.
23. Renner, C.; Behrendt, R.; Heim, N.; Moroder, L. *Biopolymers* **2002**, *63*, 382.
24. Wilner, I.; Rubin, S. *Angew. Chem.* **1996**, *108*, 419. *Angew. Chem., Int. Ed.* **1996**, *35*, 367.
25. Bandara, H. M. D.; Friss, T. R.; Enriquez, M. M.; Isley, W.; Incarvito, C.; Frank, H. A.; Gascon, J.; Burdette, S. C. *J. Org. Chem.* **2010**, *75*, 4817.
26. Maina, T.; Nock, B.; Nikolopoulou, A.; Sotiriou, P.; Maintas, G. D.; Cordopatis, P.; Chiotellis, E. *Eur. J. Nucl. Med. Mol. Imaging* **2002**, *29*, 742.
27. (a) Becker, O. M.; Levy, Y.; Ravitz, O. *J. Phys. Chem. B* **2000**, *104*, 2123; (b) Levy, Y.; Jortner, J.; Becker, O. M. *Proc. Natl. Acad. Sci. U.S.A.* **2001**, *98*, 2188–2193; (c) Levy, Y.; Becker, O. M. *J. Chem. Phys.* **2001**, *114*, 993–1009.
28. Bakker, W. H.; Krenning, E. P.; Breeman, W. A. P.; Koper, J. W.; Kooij, P. P.; Reubi, J. C.; Klijn, J. G.; Visser, T. J.; Docter, R.; Lamberts, S. *J. Nucl. Med.* **1990**, *31*, 1501.
29. Froidevaux, S.; Hintermann, E.; Török, M.; Mäcke, H. R.; Beglinger, C.; Eberle, A. N. *Cancer Res.* **1999**, *59*, 3652.
30. Raynor, K.; Reisine, T. *J. Pharmacol. Exp. Ther.* **1989**, *251*, 510.
31. Lowry, O. H.; Rosebrough, N. J.; Farr, A. L.; Randall, J. *J. Biol. Chem.* **1951**, *193*, 265.